$Cs^+(15\text{-crown-}5)_2 \cdot e^-$. A Crystalline Antiferromagnetic Electride

Steven B. Dawes, Judith L. Eglin, Kevin J. Moeggenborg, Jineun Kim, and James L. Dye*

Contribution from the Department of Chemistry and Center for Fundamental Materials Research, Michigan State University, East Lansing, Michigan 48824-1322.
Received August 2, 1990

Abstract: The crystalline electride formed from cesium metal and 15-crown-5 contains sandwiched Cs^+ cations and trapped electrons, the latter presumably centered at relatively isolated anionic sites. The magnetic susceptibility obeys the Curie–Weiss law above about 15 K, and annealed polycrystalline samples show an antiferromagnetic transition at 4.6 K. At 1.6 K, spin alignment occurs in a magnetic field and is essentially complete above 0.3 T, indicating that the magnetic anisotropy is weak. The ^{133}Cs NMR spectrum and magnetic susceptibility as a function of temperature allowed the determination of the electron density at the cesium nucleus as only 0.063% that of a free cesium atom but nearly twice that found for $Cs^+(18\text{-crown-}6)_2 \cdot e^-$. The properties and structure suggest electron localization in cavities similar to the anionic sites in $Cs^+(15\text{-crown-}5)_2 \cdot Na^-$, with relatively weak interactions among the trapped electrons.

Introduction

Electrides are crystalline salts in which the charges on complexed alkali-metal cations are balanced by trapped electrons.[1-11] Because of the light mass and consequent quantum mechanical behavior of electrons, there is considerable interest in the nature of the electron trapping, the overlap of the wave function of the trapped electron with neighboring molecules, and the interactions among electrons. Although the properties of the trapped electrons in electrides cover the range from strong overlap and near-metallic behavior[6] to nearly independent behavior,[1] most electrides synthesized to date fall into the latter category. That is, the optical, magnetic, and electrical behavior is that expected for localized electrons that interact only weakly with one another. Exceptions are $Li^+(\text{cryptand 211}) \cdot e^-$[12] and $K^+(\text{cryptand 222}) \cdot e^-$[6], which show much stronger electron–electron interactions as well as optical spectra and conductivities that are reminiscent of near-metallic behavior.

This report describes the properties of $Cs^+(15\text{-crown-}5)_2 \cdot e^-$ [$Cs^+(15C5)_2 \cdot e^-$], an electride of known structure,[11] in which the electrons are localized yet interact strongly enough to form an antiferromagnetically ordered structure below 4.6 K.

The structures of two other electrides have been published. One of these ($Cs^+(18\text{-crown-}6)_2 \cdot e^-$ [$Cs^+(18C6)_2 \cdot e^-$][3]) has localized electrons that interact only weakly with each other and with the cation. The other ($K^+(\text{cryptand 222}) \cdot e^-$[5,6]) contains *electron pairs* in a singlet ground state that lie only ~0.05 eV below the triplet (or dissociated) state. This electride is *much* more conductive (by a factor of at least 10^6) than either $Cs^+(18C6)_2 \cdot e^-$ or $Cs^+(15C5)_2 \cdot e^-$ and has an optical absorption spectrum that is suggestive of weakly bound or delocalized electrons.

A number of other crystalline electrides have been synthesized, such as $Rb^+(\text{cryptand 222}) \cdot e^-$, $Rb^+(15C5)_2 \cdot e^-$, $K^+(15C5)_2 \cdot e^-$, and $Li^+(\text{cryptand 211}) \cdot e^-$. The latter compound exhibits spin pairing[12] below about 200 K and Curie–Weiss behavior at higher temperatures. Its structure has recently been determined.[13] The others show no magnetic transitions and appear to contain unpaired localized electrons.

Experimental Section

$Cs^+(15C5)_2 \cdot e^-$ was synthesized by following a procedure that has been described in detail elsewhere.[14] Briefly, stoichiometric quantities of cesium and the crown ether were introduced into separate side arms on an evacuable borosilicate glass "K-cell". The cesium was introduced in a sealed tube into one of the side arms that had a Teflon heat-shrinkable connection to a closed-end tube. After evacuation to $\sim 10^{-5}$ Torr, the cesium-containing tube was broken by bending at the Teflon connection, the side arm was sealed off, and the cesium was vacuum-distilled into the reaction vessel. In an alternate procedure, cesium metal was introduced into the side arm in a helium-filled inert-atmosphere box, the side arm was capped by a tube and an Ultra Torr connector, and after removal from the box and evacuation the sidearm was sealed off.

Purified dimethyl ether (Me_2O) was distilled onto the 15-crown-5 sample at 230 K, and the resulting solution of the complexant was poured into the side of the K-cell that contained the Cs metal mirror. The metal dissolved rapidly to form a stable deep blue solution. Crystals were grown from this solution by adding diethyl ether (Et_2O) at 230 K and then slowly removing Me_2O by vacuum distillation. Further crystal growth was accomplished by cooling the Et_2O-rich solution to 195 K. In an alternate procedure, mixed Me_2O–Me_3N (dimethyl ether–trimethylamine) solutions were slowly cooled from 230 to 198 K to effect crystallization. Since the compound is insoluble in cold Et_2O or Me_3N, one of these solvents was used to wash the crystals free of excess crown ether. After evaporation of all the Et_2O, the product was vacuum-dried and transferred to glass ampules that were vacuum-sealed while the samples were kept at 77 K, the temperature at which they were stored until needed.

Because the electride is very sensitive to oxidation and to thermal decomposition, all manipulations were carried out under nitrogen in a glovebag while the sample was kept cold on an aluminum support immersed in liquid nitrogen. Analysis via a scheme described elsewhere[15] confirmed the stoichiometry $Cs(15C5)_2$.

Differential scanning calorimetry (DSC) was performed with a Du Pont Model 910 differential scanning calorimeter by using hermetically sealed aluminum pans and precooling the DSC to 228 K.

Optical absorption spectra of thin solvent-free films of the electride were measured from 400 to 2000 nm in a Beckman DK2 spectrophotometer at temperatures from 200 to about 275 K as recorded with a copper-constantan thermocouple. Thin films were made by preparing a solution in Me_2O, pouring the solution over the cell window, and then rapidly evaporating the solvent. Later determinations used a Guided

(1) Ellaboudy, A.; Dye, J. L.; Smith, P. B. *J. Am. Chem. Soc.* **1983**, *105*, 6490.
(2) Dye, J. L. *Prog. Inorg. Chem.* **1984**, *32*, 327.
(3) Dawes, S. B.; Ward, D. L.; Huang, R. H.; Dye, J. L. *J. Am. Chem. Soc.* **1986**, *108*, 3534.
(4) Dye, J. L. *Sci. Am.* **1987**, *257*, 66.
(5) Ward, D. L.; Huang, R. H.; Dye, J. L. *Acta Crystallogr.* **1988**, *C44*, 1374.
(6) Huang, R. H.; Faber, M. K.; Moeggenborg, K. J.; Ward, D. L.; Dye, J. L. *Nature* **1988**, *331*, 599.
(7) Dye, J. L. *Valency*, The Robert A. Welch Foundation Conference on Chemical Research XXXII, Houston, TX, 1989; p 65.
(8) Dawes, S. B.; Ward, D. L.; Fussa-Rydel, O.; Huang, R. H.; Dye, J. L. *Inorg. Chem.* **1989**, *28*, 2132.
(9) Dye, J. L. *Science (Washington, D.C.)* **1990**, *247*, 663.
(10) Dye, J. L.; Huang, R. H. *Chem. Br.* **1990**, *26*, 239.
(11) Ward, D. L.; Huang, R. H.; Kuchenmeister, M. E.; Dye, J. L. *Acta Crystallogr.* **1990**, *C46*, 1831.
(12) Landers, J. S.; Dye, J. L.; Stacy, A.; Sienko, M. J. *J. Phys. Chem.* **1981**, *85*, 1096.
(13) Huang, R. H.; Ward, D. L.; Dye, J. L. Unpublished results.
(14) Dye, J. L. *J. Phys. Chem.* **1984**, *88*, 3842.
(15) Van Eck, B.; Le, L. D.; Issa, D.; Dye, J. L. *Inorg. Chem.* **1982**, *21*, 1966.

0002-7863/91/1513-1605$02.50/0

Wave Model 260 fiber-optic spectrophotometer.

Magnetic susceptibilities were measured with an S.H.E. 800 Series SQUID magnetometer over a temperature range of 2–283 K in applied fields of 0.01–0.70 T. The background susceptibility was obtained by allowing the sample to decompose to a diamagnetic product. This procedure allows one to obtain the *electronic* portion of the susceptibility[12] (χ_e^m) and eliminates contributions from the complexant, the container, and the core electrons in Cs^+. The molar susceptibility (emu mol^{-1}) is the (total sample magnetization × molecular weight)/(magnetic field strength × sample mass). The magnetic susceptibility is reported for samples with two different thermal treatments. *Quenched* samples were rapidly cooled in helium from 250–270 to 4.5 K by loading them directly into the susceptometer. *Annealed* samples were formed by warming the quenched samples to about 230 K and then slowly cooling them in the susceptometer to 5 K before starting the measurements. The two types of heat treatments were carried out on different preparations and on the same sample.

Magic angle sample spinning (MAS) ^{133}Cs NMR spectra were obtained at 23.6 MHz with a Bruker WH180 NMR spectrometer operating at a field strength of 4.227 T, with 4–5-μs pulse lengths and 0.5–2-s delay times. A variable-temperature Doty dual-bearing MAS probe was used. The temperature was controlled by flowing the N_2 spinning gas through a liquid nitrogen heat exchanger and then warming the gas with an in-line heater. The temperature was monitored with a thermocouple placed in the gas stream before it entered the spinner.

It proved to be difficult to determine the actual sample temperature. At first, alternate measurements of the electride sample and the dipolar splitting of methanol protons[16,17] were used with constant gas flow and heater power settings. A second method used a rotor filled with a mixture of $Cs^+(15C5)_2{\cdot}e^-$ and $Cs^+(18C6)_2{\cdot}e^-$, the latter having a known temperature dependence of the chemical shift.[18] Additional signals appeared, indicating the presence of a solid-state reaction between the pure electrides, probably to form the mixed-sandwich compound. Finally, the Kel-F bolt used to attach the end caps to the sapphire rotor was modified by sealing a sample of methanol inside a hole drilled lengthwise into its center. In this way, alternate ^{133}Cs and ^1H measurements could be made without the rotor being removed from the instrument. This method provided a reliable and reproducible measurement of the sample temperature. However, the presence of temperature gradients within the sample holder could not be ruled out.

Static NMR measurements were also carried out at 52.5 MHz in a Varian VXR-400 spectrometer with a 45–165 MHz broad-band probe with single pulses of width 0.5 μs and delay time of 0.5 s. Cold nitrogen gas was used to control the temperature to within ±0.3 K after 3–10-min equilibration time.

The dc conductivity of packed powders of $Cs^+(15C5)_2{\cdot}e^-$ was measured as a function of temperature (130–270 K) and voltage (up to ±5 V) with a Keithley 617 programmable electrometer. To eliminate pronounced deviations from Ohm's law due to electrode effects, the electrodes were coated with cesium metal. Impedance spectroscopy measurements at 240–300 K over the frequency range 5 Hz to 13 MHz were made with a Hewlett-Packard 4192A-LF impedance analyzer. The sample temperature was controlled by adjusting the position of the sample in a liquid N_2 dewar. Temperature stability to ±0.1 K and the absence of significant temperature gradients were verified by placing thermocouples near the bottom and the top of the sample.

Results

Structural Overview. Details of the crystal structure of $Cs^+(15C5)_2{\cdot}e^-$ are reported elsewhere.[11] It belongs to the triclinic space group $P\bar{1}$ with one molecule per unit cell and the following cell parameters: a = 8.597 (4), b = 8.886 (8), and c = 9.941 (9) Å; α = 102.91 (8), β = 90.06 (6), and γ = 97.74 (6)°; V = 733.1 (11) Å^3; and ρ = 1.30 g cm^{-3}. The structure was determined at a temperature of 215 ± 2 K.

The cesium cation is located in the center of a 15-crown-5 sandwich with normal Cs^+–O distances that range from 3.080 to 3.298 Å. The electron density due to the trapped electron is too low to observe by X-ray diffraction, but it is presumably centered in the anionic site. This is a cavity located at the inversion center ($^1/_2$, $^1/_2$, $^1/_2$). The closest distance from this center to adjacent hydrogens is 3.25 Å, and the average distance to the 10 nearest hydrogens is 3.55 Å. This implies a minimum cavity diameter

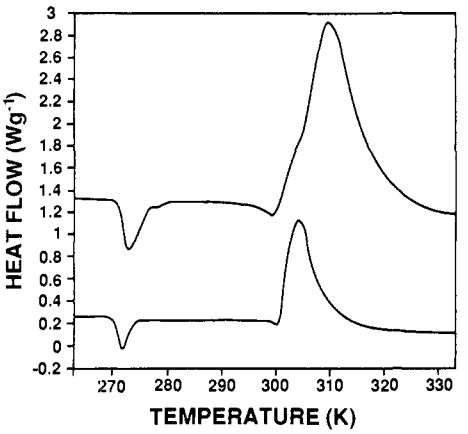

Figure 1. Differential scanning calorimetry (DSC) traces of $Cs^+(15C5)_2{\cdot}e^-$ at ramping rates of 2 K min^{-1} (lower trace) and 5 K min^{-1} (upper trace, offset by 1 W g^{-1}).

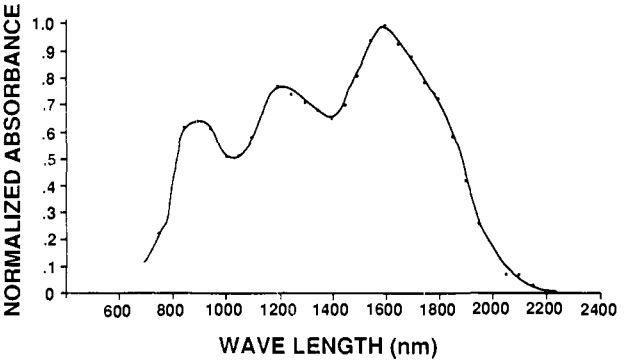

Figure 2. Optical absorption spectrum of a thin film of $Cs^+(15C5)_2{\cdot}e^-$ prepared by evaporating dimethyl ether from a solution of $Cs^+(15C5)_2{\cdot}e^-$.

of about 4.0 Å and a mean diameter of 4.7 Å measured to the hydrogen van der Waals surfaces. The corresponding sodide $Cs^+(15C5)_2{\cdot}Na^-$ is isostructural and has Na^- ions in the sites that are "empty" in the electride.[13] Each anionic site in the electride is surrounded by eight nearest-neighbor complexed cesium cations, two each at distances of 6.92, 7.63, 8.23, and 8.38 Å and is connected by rather constricted channels to six equivalent sites at distances of 8.60, 8.89, and 9.94 Å (two at each distance).

Thermal Behavior. Below about 260 K, powdered samples of the electride are polycrystalline and can be readily transferred from one container to another by pouring. As the temperature is increased (particularly above 266 K), the sample becomes "sticky" but it remains solid. At about 295 K, the compound melts to give a deep blue liquid that decomposes rapidly and irreversibly.

As shown in Figure 1, differential scanning calorimetry reflects these changes in behavior. A pronounced endotherm at 266 K corresponds to ΔH = 11.2 ± 0.6 kJ mol^{-1} and is reversible. That is, cooling a sample that had been warmed to 283 K in the DSC to 230 K gave the same endothermic transition during the second cycle. The melting transition at ~295 K (observed at a scan rate of 10° min^{-1}) was followed by a large exothermic peak due to irreversible decomposition. At slower scan rates (1° min^{-1}), the exothermic peak obscured the endothermic peak of melting.

Optical Spectra. The absorption spectra of thin films of $Cs^+(15C5)_2{\cdot}e^-$ are more complex than those of most other electrides. Usually, a single broad absorption is observed in the near-IR region at 1200–1600 nm.[1,19] Alkalide films show the single absorption band of M^-.[20] When solvent-free films are prepared from solutions that contain *both* solvated electrons and alkali-metal anions, however, new absorption peaks are often

(16) Van Geet, A. L. *Anal. Chem.* **1970**, *42*, 679.
(17) Yamamoto, O.; Yanagisawa, M. *Anal. Chem.* **1970**, *42*, 1463.
(18) Dawes, S. B.; Ellaboudy, A. S.; Dye, J. L. *J. Am. Chem. Soc.* **1987**, *109*, 3508.
(19) DaGue, M. G.; Landers, J. S.; Lewis, H. L.; Dye, J. L. *Chem. Phys. Lett.* **1979**, *66*, 169.
(20) Dye, J. L.; Yemen, M. R.; DaGue, M. G.; Lehn, J.-M. *J. Chem. Phys.* **1978**, *68*, 1665.

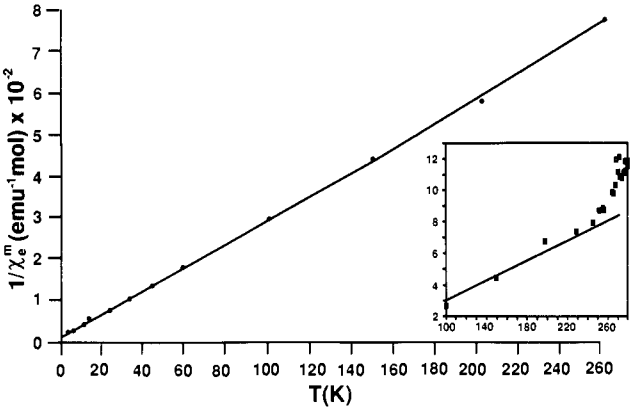

Figure 3. Magnetic susceptibility data ($1/\chi_e^m$ versus temperature) for $Cs^+(15C5)_2\cdot e^-$ with an inset that shows the high-temperature data.

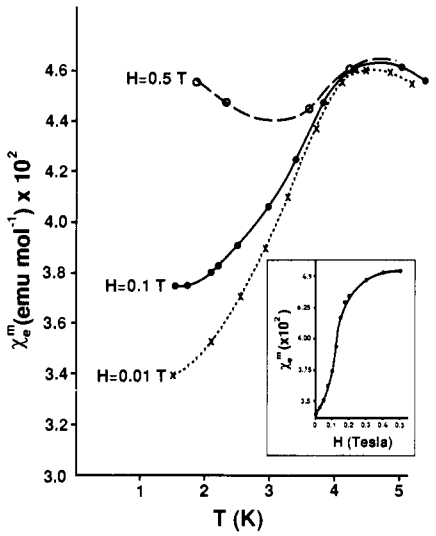

Figure 4. Magnetic susceptibility of an annealed sample of $Cs^+(15C5)_2\cdot e^-$ below 5 K at different fields. The inset shows the field dependence of the magnetic susceptibility at 1.6 K.

observed in addition to those of M^- and e^-.[21] The spectra of films of $Cs^+(15C5)_2\cdot e^-$, prepared by evaporating methylamine from a solution of the electride, have as many as three absorption peaks whose relative intensities depend on the preparation. As shown in Figure 2, these peaks are at 900–950, ~1250, and 1600–1700 nm. Later preparations showed the same three peaks. One film showed reversible temperature behavior. The peak at 950 nm was pronounced at 270 K (just above the transition temperature), disappeared at 240 K, and reappeared again upon warming. At the lower temperature, a single broad peak at ~1400 nm was present with, however, shoulders at both lower and higher wavelengths. The variability of the optical spectrum from one preparation to the next is common when multiple peaks are present because of possible variations in the composition and orientation of the crystallites in the film.

Magnetic Susceptibility. The magnetic susceptibility of $Cs^+(15C5)_2\cdot e^-$ was studied over the temperature range 1.6–283 K and at field strengths from 0.01 to 0.7 T. Samples that were quenched by sudden cooling to 5 K showed the same behavior above this temperature as those that were "annealed" for a few minutes at ~230 K followed by slow cooling. The Curie–Weiss behavior is shown in Figure 3, while the inset shows the susceptibility in the region of the 266 K phase transition. A least-squares fit to the data from 5 to 260 K of the equation $\chi_e^m = C/(T-\Theta) + B$ yielded $C = 0.361$ emu mol^{-1} K, $\Theta = -4.5$ K, and $B = -1.2 \times 10^{-4}$ emu mol^{-1}. In contrast to quenched samples, which showed

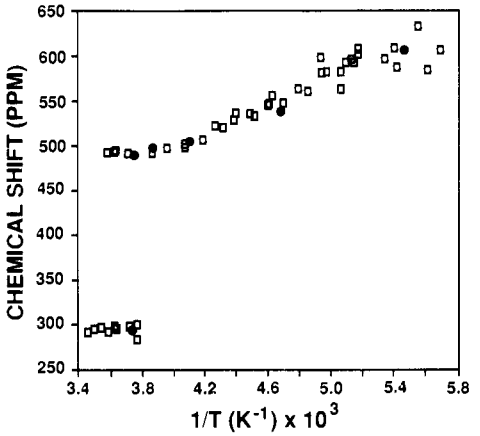

Figure 5. ^{133}Cs NMR chemical shift versus $1/T$ for $Cs^+(15C5)_2\cdot e^-$, 180-MHz MAS NMR data (open squares), and 400-MHz static data with the isotropic chemical shift obtained from simulations of the experimental powder patterns (circles).

nearly Curie–Weiss behavior below 5 K, annealed samples yielded a maximum in the susceptibility at 4.6 K. Because of a slight mismatch between the low-temperature (<5 K) and high-temperature (>5 K) susceptibility data, the low-temperature data were shifted uniformly to provide continuity in the region of overlap.

As demonstrated in Figure 4, the susceptibility data show that an antiferromagnetic transition occurs at about 4.6 K and that the susceptibility is field-dependent below this temperature. The inset shows that the anisotropy is relatively weak, since a field of only 0.3 T is sufficient to cause a "spin-flop"; that is, the axis of antiferromagnetic alignment, originally randomly oriented so that the limiting susceptibility at 0 K is two-thirds of that at the maximum,[22] "flops" in the presence of a field so that alignment occurs along another axis and the susceptibility increases with increasing field to that of the perpendicular component, essentially the same value as at the Néel temperature. At temperatures well above the Néel temperature, the susceptibility follows the Curie–Weiss law. However, at about 260–265 K (just below the temperature of the endothermic transition seen in the DSC experiments) the slope of a plot of $1/\chi$ vs T changes in a direction that corresponds to less paramagnetism (Figure 3 inset). Whether an abrupt change in susceptibility accompanies the phase transition cannot be ascertained from the susceptibility data since the sample temperature in the SQUID susceptometer tends to overshoot before coming to equilibrium. Thus, partial conversion to a less paramagnetic high-temperature form could have occurred. As described below in connection with NMR studies, the conversion can be slow so that a mixture of the two phases could result. Also at the temperature of the phase transition, some decomposition can occur, which tends to make the sample less paramagnetic. Correction for irreversible decomposition was made for each pass through the phase transition by comparison of the low-temperature susceptibility with that of a fresh sample.

^{133}Cs NMR Spectra. A large number of NMR experiments have been carried out on $Cs^+(15C5)_2\cdot e^-$, including MAS spectra at 23.6 MHz and static spectra at 52.5 MHz at temperatures between 176 and 290 K. Both the early MAS measurements, which were flawed by difficulty in measuring the sample temperature, and later MAS measurements with more accurate temperature calibration showed two peaks with chemical shifts of 490 and 290 ppm. Both peaks were present over the apparent temperature range 265–280 K, each at a constant value of the chemical shift as shown in Figure 5. When the temperature was raised above 280 K, only the peak at 290 ppm was present. These measurements had to be made rather rapidly to avoid decomposition, a process that could be monitored by the growth of a peak of the decomposition products at 61 ppm. Since the DSC results showed a reversible endothermic transition at 266 K, we surmised

(21) Dye, J. L.; DaGue, M. G.; Yemen, M. R.; Landers, J. S.; Lewis, H. L. *J. Phys. Chem.* **1980**, *84*, 1096.

(22) Carlin, R. L. *Magnetochemistry*; Springer-Verlag: Berlin, 1986.

that the phase transition was not complete in the NMR rotor during the measurement time and that the actual sample temperature may have been constant even though the temperature of the spinning gas continued to increase. That this was indeed the case was shown by studying the time dependence of the static spectrum at 266 K. Over a 120-min period, the static peak with an isotropic chemical shift of 488 ppm decayed, while that at 294 ppm grew in. Rapid cooling to 253 K caused reversal of the process over a period of 3–5 min. These results are in complete agreement with the DSC data and confirm the presence of a first-order phase transition at 266 K.

The static ^{133}Cs NMR spectra at 52.5 MHz were also obtained as a function of temperature. Typical Gaussian broadened powder patterns arising from chemical shift anisotropy (CSA) were obtained. The isotropic chemical shift ranged from 604 ppm at 183 K to 496 ppm at 258 K, in excellent agreement with that obtained from MAS NMR measurements at 23.6 MHz (Figure 5). The anisotropy parameter (η for CSA) was 0.3 ± 0.05. The required Gaussian broadening corresponded to full widths at half-maximum that ranged from 3.3 ± 0.2 kHz at 183 K to 1.5 ± 0.1 kHz at 243 K. Since the proton dipolar broadening as calculated from the crystal structure with the Van Vleck equation[23] is only 1.1 kHz and typical values for model salts[24] are 0.4–0.7 kHz, we attribute much of the broadening to incompletely relaxed electron–nucleus dipolar coupling. The rigid-lattice limit for such coupling is 57.4 kHz. Clearly, electron spin–lattice relaxation averages out most, but not all, of the electron–nucleus coupling, and the residual effect is strongly temperature-dependent.

Below about 240 K, the chemical shift is linear in $1/T$, with an intercept of 180 ± 10 ppm and a slope of 7.9 ± 0.5 × 10^4 ppm K. (The uncertainties are standard deviation estimates.) The intercept is about 150 ppm higher than that obtained for model salts that contain the $Cs^+(15C5)_2$ cation.[24] The slope corresponds to a contact density at Cs^+ that has 0.063% atomic character, nearly twice that found for $Cs^+(18C6)_2{\cdot}e^-$.[18] The rather large anisotropy in the Cs^+ to e^- distances suggests that the contribution to the contact density is probably different for different electrons.

Electrical Conductivity. Impedance spectroscopy and dc conductivity studies of three electrides will be described in detail elsewhere,[25] so only a brief description of the behavior of $Cs^+(15C5)_2{\cdot}e^-$ will be given here. This electride is essentially an insulator that shows only conductivity due to defect electrons below about 190 K. The magnitude of this conductivity depends upon the preparation as does the activation energy. For example, three different preparations gave values of the specific conductance at 180 K that ranged from 5 × 10^{-8} to 2 × 10^{-11} S cm, while the activation energies varied from 0.14 to 0.18 eV. At higher temperatures, impedance spectroscopy, time-dependent polarization and its elimination with cesium-coated electrodes, and the behavior upon charge–discharge cycles all suggest that the conductivity is largely ionic in nature with an activation energy of about 0.6 eV. We conclude that $Cs^+(15C5)_2{\cdot}e^-$ is electronically an insulator with a band gap of at least 1.0 eV.

Discussion

The crystalline electride $Cs^+(15C5)_2{\cdot}e^-$ consists of sandwiched cesium cations, packed closely together in a manner that could be roughly described as a distorted body-centered cubic lattice with a cavity at the center. In the isostructural sodide, the Na^- ion occupies this central cavity. The "normal" geometry and Cs–O distances in the complex and the small electron-spin density at cesium strongly suggest that the excess electron density is centered in the anionic sites with, however, probable extension of the wave function beyond the van der Waals boundaries of the cavity. Clearly, the electrons are localized, with ground-state energies at least 1.0 eV below the conduction band, as indicated by the absence of detectable intrinsic electronic conductivity below 190 K.

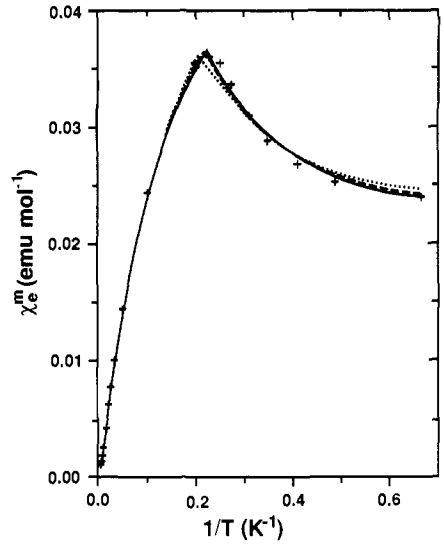

Figure 6. Fit of the magnetic susceptibility of $Cs^+(15C5)_2{\cdot}e^-$ with the equations of Ohya-Nishiguchi (solid line), Oguchi (dashed line), and mean-field theory (dotted line).

The optical absorption spectrum of thin films produced by solvent evaporation is complex, consisting of at least three peaks at 900–950, ~1250, and 1600–1700 nm, with the highest energy peak predominating at temperatures above the first-order transition at 266 K. A possible explanation is that the optically allowed transitions are of the s to p type and that the three excited p states have rather different energies because of different degrees of overlap with neighboring Cs^+ ions.[26] These ions are located at distances that range from 6.92 to 8.83 Å. It is also possible that the peak at 900 nm (1.4 eV) results from a bound-continuum transition. However, the difficulty in producing a uniform film by solvent evaporation makes truly quantitative absorption spectra unattainable, so that any explanation must remain tentative until better absorption or reflectance spectra become available.

Carefully annealed samples of $Cs^+(15C5)_2{\cdot}e^-$ are antiferromagnetic with a Néel temperature of 4.6 K. As shown in Figure 6, the data can be reasonably well-fit over the entire temperature range from 1.5 to 260 K with use of simple mean-field theory,[27] the mean-field theory of Oguchi,[28] or its modification by Ohya-Nishiguchi.[29] The latter modification considers explicit magnetic coupling of a pair of spins and weaker coupling to other spins, the other spins being treated by the mean-field approximation. Because of an error in the expression for $\chi_\perp$ in the original Oguchi paper[28] and several minor misprints in the published Ohya-Nishiguchi equation,[29] the corrected equations are given below. The parameters were adjusted with the nonlinear least-squares program KINFIT[30] and the susceptibility calculation program ANTIMAG.[31] The final equations of Ohya-Nishiguchi are as follows

$$\chi_\parallel = \frac{Ng^2\mu^2\beta}{2[-\kappa\beta J + 1 + e^{-\beta J}\cosh(\beta JR)]} \quad (1)$$

$$\chi_\perp = \{Ng^2\mu^2[(1-R)^2e^{-\beta J}\cosh(\beta JR) + 2R - (R^2+1)e^{-\beta J(1-R)}]\}/\{[-2J\kappa(1-R)^2e^{-\beta J}\cosh(\beta JR) + 2R - (R^2+1)e^{-\beta J(1-R)}] + 2JR(1-R^2)[1+e^{-\beta J}\cosh(\beta JR)]\} \quad (2)$$

where $\beta = 1/kT$, $\kappa = (J'/J)(z-1)$, and R is the root of the following self-consistent equation:

$$R[e^{\beta J} + \cosh(\beta JR)] + \kappa\sinh(\beta JR) = 0.$$

The number of nearest neighbors to a given paramagnetic center,

(23) Van Vleck, J. H. *Phys. Rev.* **1948**, *74*, 1169.
(24) Kim, J.; Ellaboudy, A. S.; Dawes, S. B.; Dye, J. L. Unpublished results.
(25) Moeggenborg, K. J.; Dye, J. L. Unpublished results.
(26) We are indebted to Prof. H. B. Gray for pointing out this possibility.
(27) Smart, J. *Effective Field Theories of Magnetism*; W. B. Saunders Co.: Philadelphia, 1966.
(28) Oguchi, T. *Prog. Theor. Phys.* **1955**, *13*, 148.
(29) Ohya-Nishiguchi, H. *Bull. Chem. Soc. Jpn.* **1979**, *52*, 3480.
(30) Dye, J. L.; Nicely, V. A. *J. Chem. Educ.* **1971**, *48*, 443.
(31) Kim, J. Ph.D. Dissertation, Michigan State University, East Lansing, MI, 1989.

Table I. Best Fit Parameters: Molar Electronic Susceptibility of $Cs^+(15C5)_2\cdot e^-$ [a]

equation	other	J/k (K)	θ (K)	T_N (K)	f (%)	B (emu mol^{-1})
Oguchi	$z = 6$, $J' = J$	−1.61 (1)	−4.83 (5)	4.64	95.5 (8)	$-1.2\ (3) \times 10^{-4}$
Ohya-Nishiguchi	$\kappa = 4.0$ (4)	−1.9 (2)	−4.78 (5)	4.51	95.9 (9)	$-1.3\ (3) \times 10^{-4}$
mean-field	$z = 6$, $J \ll J'$	−1.63 (2)[b]	−4.89 (6)	4.89	94.7 (13)	$-1.0\ (5) \times 10^{-4}$

[a] Uncertainties given in parentheses are standard deviation estimates of the last digit. [b] For the mean-field case, this is J'/k.

including the other member of the pair, is z (defined as $z - 1$ in the Ohya-Nishiguchi paper). J is the intrapair interaction energy, and J' is the interaction energy between a paramagnetic species in the pair and one of the other $z - 1$ neighbors to this center. For $J' = J$, the Ohya-Nishiguchi equations reduce to the Oguchi equations. The simple mean-field expression is obtained by setting J to an extremely small value.

The powder susceptibility at low field is given by $\chi = (\chi_\parallel + 2\chi_\perp)/3$. A diamagnetic term ($B$) was also included. The results obtained by fitting these equations to the data are given in Table I. Note particularly that essentially all (96%) of the electrons contribute to the susceptibility. The fit of the data is shown in Figure 6. The close correspondence of all models results from the fact that the best fit value of J'/J is not very different from unity, corresponding to nearly equal coupling to all six adjacent electrons. Although annealing establishes a natural "easy axis" of magnetization, the anisotropy is not large and at 1.6 K a field of only 0.3 T suffices to "flop" the spins to the lower energy perpendicular arrangement.

This is the only electride synthesized to date that exhibits an antiferromagnetic transition, although some others have large negative values of the Weiss constant (Θ). For example, $K^+(15C5)_2\cdot e^-$ has $\Theta = -20.4 \pm 0.6$ K but shows neither a transition nor field dependence.[32] Perhaps the explanation lies in the simplicity of the crystal structure of $Cs^+(15C5)_2\cdot e^-$. With only one molecule per unit cell it is a relatively simple matter to form an antiferromagnetic superlattice via nearest-neighbor interactions only. The presence of a spin-flop that saturates at fields of ~0.3 T at 1.6 K implies rather weak anisotropy of the coupling constant J (of the order of 10–15%). The origin of this anisotropy is probably the difference in electron–electron distances along the a, b, and c axes. This distance increases by 3.5% from a to b and by 16% from a to c.

The endothermic transition at 266 K is accompanied by a decrease in paramagnetism, but the sluggishness of the transition, the competition from irreversible decomposition, and the tendency of the temperature of the susceptometer to overshoot make it difficult to distinguish between a discontinuity in the susceptibility and a change in the slope of $1/\chi$ vs T. We can conclude, however, that the electronic susceptibility 10 K above the transition is about 60% of the value 10 K below it. The chemical shift of the ^{133}Cs NMR signal decreases abruptly from 493 ppm below the transition temperature to 294 ppm above this temperature. The most likely cause of this change is the decrease in the magnetic susceptibility. For a constant value of the unpaired spin density at Cs^+, the chemical shift from that of a diamagnetic model salt is directly proportional to the susceptibility. Model compounds that contain the $Cs^+(15C5)_2$ sandwich structure have chemical shifts of 30 ± 5 ppm.[25] The percent decrease in the paramagnetic contribution to the chemical shift at the transition (43%) is very close to the 40% decrease in susceptibility. Thus, we conclude that the transition to the higher temperature phase is accompanied by partial electron spin-pairing.

The accompanying physical change to a soft, "sticky" solid suggests that partial melting occurs, perhaps involving considerable motion of the crown ethers. The presence of increased molecular motion as the temperature is increased is demonstrated by the powder X-ray diffraction as the temperature is increased.[33] At 233 K, most of the lines have disappeared. This phenomenon is reversible, indicating that it is not caused by decomposition or the permanent formation of an amorphous phase.

The molar enthalpy change for the transition is 11.2 kJ mol^{-1}. Glass formation prevents the direct determination of the heat of fusion of 15C5. However, both 12C4 and 18C6 can be crystallized and have heats of fusion of 20 ± 1 and 38 ± 2 kJ mol^{-1}, respectively. The average (28 kJ mol^{-1}) is assumed to be approximately the heat of fusion of 15C5. Thus, the observed transition for $Cs^+(15C5)_2\cdot e^-$ has a value of ΔH that is about 20% of that expected for complete melting of 2 mol of 15C5.

A remaining puzzle is the high value (180 ppm) of the extrapolated chemical shift of the low-temperature phase as well as the curvature of a plot of the shift vs $1/T$. This contrasts with the chemical shift behavior of $Cs^+(18C6)_2\cdot e^-$ whose intercept at infinite temperature is the same as that of a diamagnetic model compound.[18] It should be noted, however, that $Cs^+(18C6)_2\cdot e^-$ also showed two NMR peaks whose relative intensities depend upon temperature. The high intercept in the present case may reflect a gradual increase in the contact density at Cs^+ that accompanies the increased motion of the crown ethers.

In summary, $Cs^+(15C5)_2\cdot e^-$ is a complex substance in which the low-temperature crystalline form has relatively isolated localized electrons trapped at all of the anionic sites and bound by a least 1.0 eV. Interactions between a trapped electron and its six nearest-neighbor trapped electrons are weak but sufficient to stabilize an antiferromagnetic superlattice below 4.6 K. Above this temperature, Curie–Weiss behavior persists to 260 K, although molecular motions become pronounced at temperatures well below this value. At 266 K, a first-order phase transition occurs that is accompanied by partial electron spin-pairing and a pronounced softening of the material. Finally at about 295 K, the compound melts and rapidly decomposes. Although the structure and properties of the low-temperature phase are known and reasonably well understood, the nature of the phase transition and the mechanism of electronic spin-pairing and of ionic conduction are unknown and require further study.

Acknowledgment. This research was supported in part by U.S. National Science Foundation Solid-State Chemistry Grants DMR 87-14751 and 87-17763 and by the Michigan State University Center for Fundamental Materials Research. We thank Drs. Rui Huang and Donald Ward for information about the crystal structure. We also thank Professor H. Ohya-Nishiguchi for providing the original derivations of his equations.

(32) McMills, L. E. H. Ph.D. Dissertation, Michigan State University, East Lansing, MI, 1989.

(33) Doeuff, S.; Tsai, K.-L.; Dye, J. L. *Inorg. Chem.*, in press.